Electrochimica Acta, Vol. 32, No. 11, pp. 1649–1654, 1987.
Printed in Great Britain.

0013–4686/87 $3.00 + 0.00

SHORT COMMUNICATION

SEM MICROGRAPHY AND VOLTAMMETRIC RESPONSE OF POLYFACETED AND ELECTROCHEMICALLY FACETED SINGLE CRYSTAL RHODIUM ELECTRODES

J. CANULLO, E. CUSTIDIANO, R. C. SALVAREZZA and A. J. ARVIA*

Instituto de Investigaciones Fisicoquímicas Teóricas y Aplicadas (INIFTA), Facultad de Ciencias Exactas, Universidad Nacional de La Plata, Casilla de Correo 16, Sucursal 4, (1900) La Plata, Argentina

(*Received* 20 *January* 1987; *in revised form* 8 *April* 1987)

INTRODUCTION

The electrochemical data reported in the literature on Rh electrodes is relatively scarce as compared to other noble metals such as Pt and Au[1–6]. Correspondingly, there are no unquestionable reference single crystal (sc) Rh systems available for establishing a direct correlation between the voltammetric response and the type of crystallographic face as for Pt and to some extent also for Au.

Recently, electrochemical faceting of polycrystalline (pc) Rh in acids has been used for the development of crystallographic faces with a definite preferred orientation[7, 8]. This technique allows to have reproducible Rh electrode surfaces which one may attempt for the first time to correlate to scanning electron microscopy (SEM) images, voltammetric response for H-atom electroadsorption–electrodesorption and underpotential deposition (upd) of Cu.

Rh spherical polyfaceted single crystal (pfsc) electrodes of about 0.8 mm diameter were made following a variation of the technique developed by Clavilier for Pt electrodes[9], that is by melting the end of a 0.5 mm diameter wire with a small oxygen gas torch flame, followed by cooling in air instead of quenching in water as proposed on the original technique.

The preparation of reproducible preferred oriented single crystal (posc) Rh electrodes started from a pfcs Rh spherical electrode immersed in 0.5 M H_2SO_4 subjected to a repetitive square wave potential (RSWP) for 3 h covering from 0.10 V (*vs rhe*) to 1.20 V range at $f = 5$ kHz. The symmetry and distribution of principal crystallographic poles of the resulting Rh surfaces and the development of preferred orientation were followed through optical and SEM microscopy, and conventional voltammetry.

Due to the fact that the voltammetric behavior of Rh in acid is to some extent comparable to that of Pt[1, 10, 11] the development of preferred orientation characteristics was tentatively followed through voltammetry for both, the H-atom electroadsorption–electrodesorption in 0.5 M H_2SO_4 and Cu upd in 0.5 M $H_2SO_4 + 10^{-3}$ M $CuSO_4$ in a conventional electrochemical cell comprising a Rh working electrode, a large Rh wire counter-electrode and a Pt reversible hydrogen electrode in 0.5 M H_2SO_4 (*rhe*) as reference electrode placed in a separate compartment. In the case of posc Rh, the voltammograms were run on electrodes which were removed at 0.1 V (oxide free surface) at the end of the RSWPS treatment.

The SEM image of the pfsc Rh surface (Fig. 1a) shows symmetrically distributed [111], [100] and [110] crystallographic poles according to the estereographical distribution of atoms at the fcc lattice (Fig. 1b). The electrode surface appears very smooth up to a magnification limit of 40000 X. On the other hand, after the electrochemical treatment, a new pattern at the Rh surface is seen (Fig. 2). The new pattern can be directly associated with an idealized scheme of the surface (Fig. 2c) which consists of a [100] direction top view of a plane projection of a hemispherical surface which exhibits a clover leaves pattern at the top with a fourfold axial symmetry axis. Then, running to the border, the pattern becomes progressively distorted. The electrochemical treatment develops univocal changes on the entire surface as it was previously reported for sc Pt spherical electrodes[12]. These changes correspond to particular faceting in such a way that, for example, the preferred orientation [100] results in a sort of "digitalized" curved surface comprising always planes parallel to the (100) face family and in the broadening of the corresponding (100) poles surfaces maintaining their flatness. A similar description can be made for other preferred orientations. This means that one way to identify crystallographic faces of indexes greater than (100), (110) and (111) after the electrochemical treatment can be based on inspecting which poles remain flat and looking around for the faceted pattern which is coherent with the geometry of those poles. Thus, from the geometric pattern of the sc spherical Rh surface resulting from SEM images it can be concluded that in the example illustrated in Fig. 2b, the preferentially developed crystallographic poles can be assigned to [610] which are located at about 9° from [100] direction. This means that either a Rh(*s*) = [5(100)

*Author to whom correspondance should be addressed.

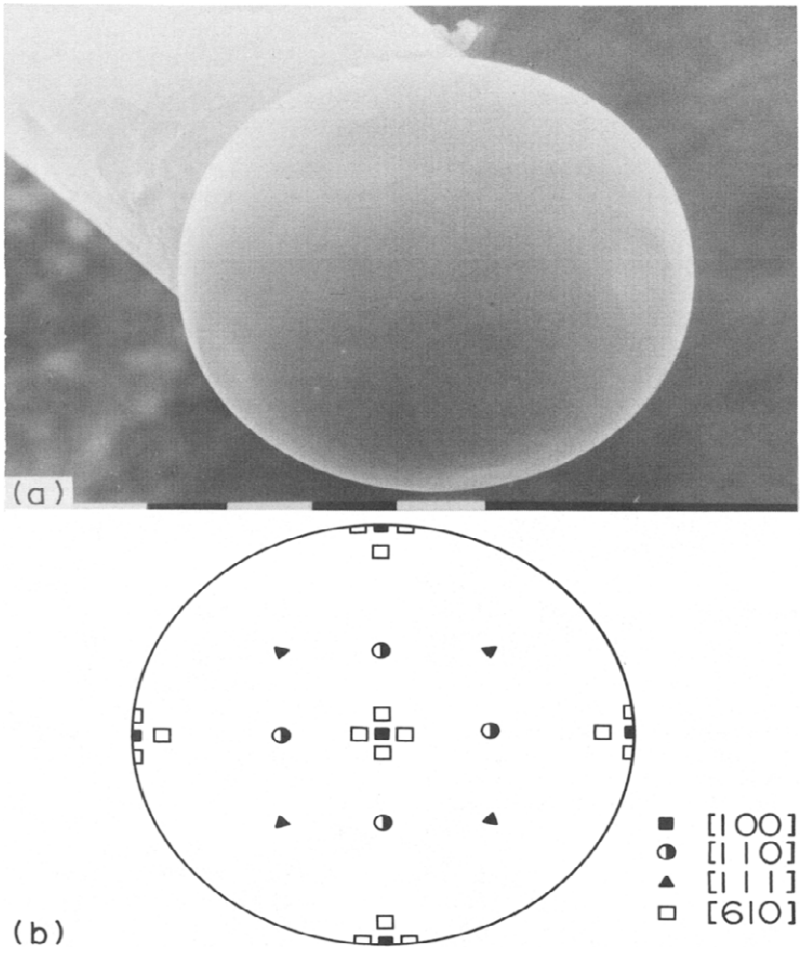

Fig. 1. (a) SEM image of pfsc Rh electrode surface. The flat circular areas corresponds to [111] poles. Scale 0.1 mm. (b) Scheme of the principal family of poles on the spherical pfsc Rh surface.

$\times$ (110)] or Rh(s) = [6(100) $\times$ (100)] array of Rh atoms at the surface[13] has been obtained. The geometry around the [610] pole (Fig. 3a) can be made from the three interwaving edge lines resulting by going from the [100] pole family to [110] pole family. The interwaving lines are parallel to two adjacent sites of the [610] pole and to one side of the [100] pole. The basis for building up this pattern is schematically shown in Fig. 3b where the intersecting edges of steps originate triangular shaped figures, in agreement with the corresponding SEM images (Fig. 3a). SEM images shown in Figs 2a, b also exhibit pitting-like defects at the [111] poles. According to the mechanism operating during the electrochemical faceting[14] it is likely that point defects at the [111] pole surfaces participate as active sites for preferred electrodissolution of Rh.

The first voltammogram of a pfsc Rh in 0.5 M H_2SO_4 at 0.1 $V s^{-1}$ between 0.03 and 0.3 V shows a single pair of reversible although slightly distorted peaks for H-adatom, the cathodic peak being located at 0.08 V and the anodic peak at 0.11 V (Fig. 4a). This asymmetry in the shape of the peaks can be attributed to an additional faradaic contribution appearing as humps at the positive potential side of both peaks. Similar runs made with posc Rh (Fig. 4b) show a more complex voltammogram consisting of a H-atom electroadsorption peak at 0.09 V and the complementary one at 0.13 V. Besides faradaic contributions appearing as shoulders at the negative potential side of both the anodic and the cathodic main peaks can be seen. Under comparable experimental conditions a clear shift in the peak potentials towards more positive values can be observed for posc electrodes. The potential of the H-adatom desorption peak at 0.15 V coincides with that reported in the literature for the Rh(100) sc electrodes[5, 6].

On the other hand, the voltammograms for the posc Rh electrodes change along the potential scan at 0.1 $V s^{-1}$ to approach progressively that of the pfsc electrode (Fig. 4c, d), namely, the faradaic contributions at lower potential increase at the expenses of those appearing earlier at higher potentials, which

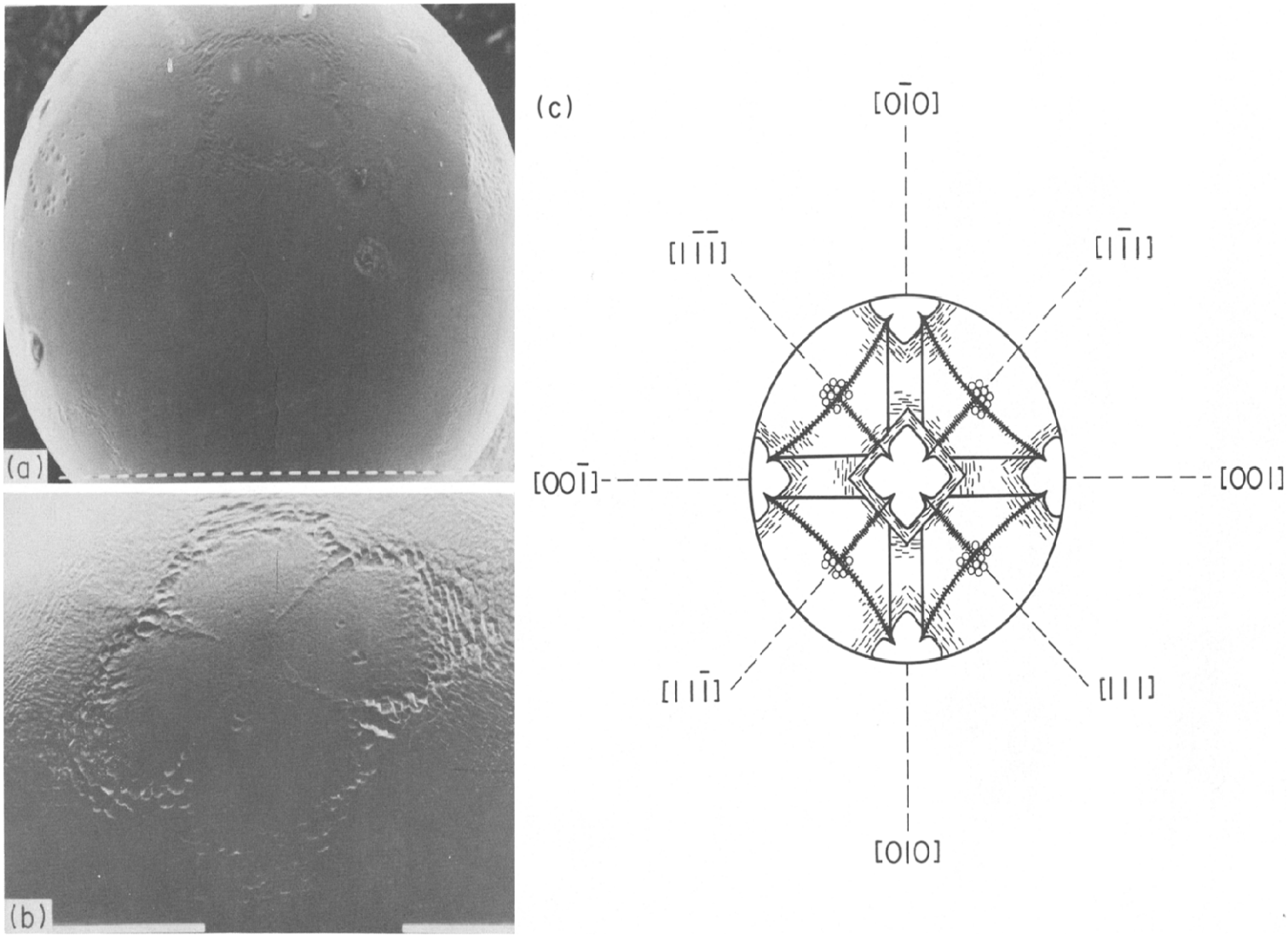

Fig. 2. (a) SEM image of posc Rh electrode surface. Scale 10 μm. (b) Detail of the [610] poles developed in the neighborhood of the [100] poles. Scale 0.1 mm. (c) Top view in the [100] direction of the symmetry pattern of a hemispherical surface comprising [610] poles.

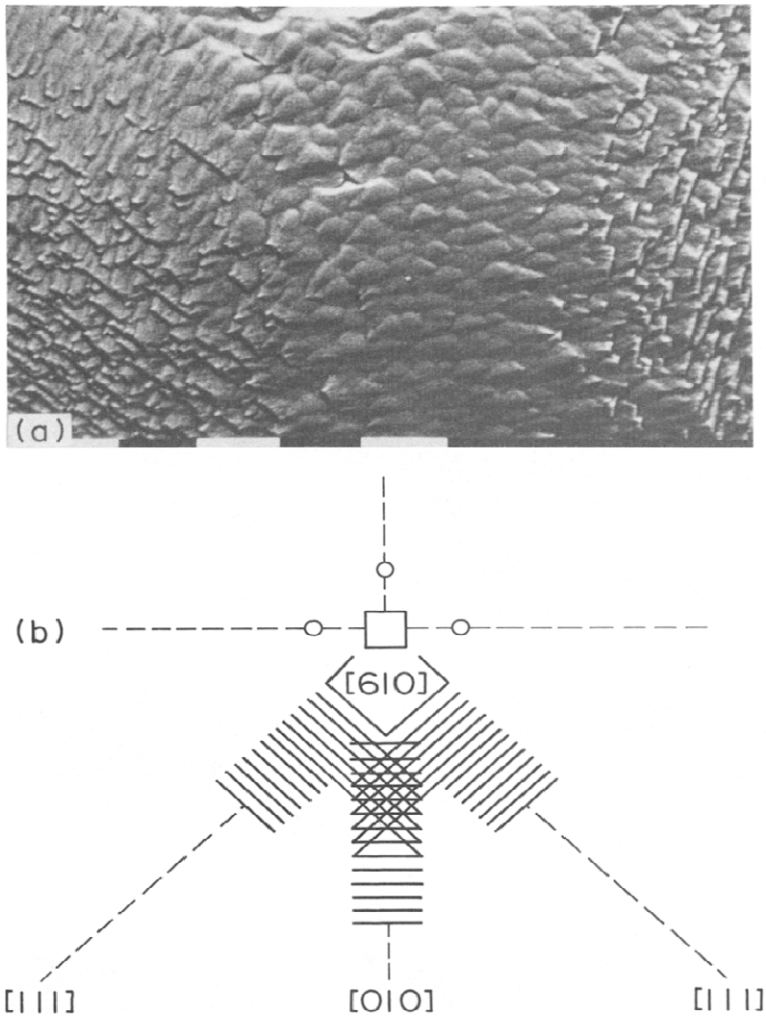

Fig. 3. (a) SEM image corresponding to a surface zone between the [610] and [010] poles. Scale 10 μm. (b) Building up scheme of interwaving macrostep borders.

according to the literature[5, 6] characterize Rh (100) faces.

The initial voltammogram of posc Rh in the H-adatom region can, therefore, principally be assigned to that of (610) crystallographic faces. In principle, as those faces are represented by the Rh(s) = [5(100) × (110)] array one should expect for them a voltammetric behaviour very close to that of Rh (100) crystallographic faces. However, a gradual reconstruction of the posc Rh occurs during the potential cycling leading progressively to voltammograms similar than those recorded for pfsc Rh.

The first voltammogram run with pfsc Rh in 0.5 M $H_2SO_4 + 10^{-3}$ M $CuSO_4$ at 0.02 V s^{-1} from 0.75 to 0.17 V shows a cathodic hump (Ic) in the 0.50 to 0.25 V range followed by a continuously increasing cathodic current up to $E_{s,c}$ (IIc) (Fig. 5a). Otherwise, the following reverse potential exhibits 3 anodic current contributions characterized by a sharp peak at 0.26 V (IIa), a broad peak at 0.46 V (I'a) and a small poorly defined peak at 0.60 V (peak I"a).

As the reversible potential (E_r) for the Cu^{2+}/Cu electrode in this solution is 0.25 V, peak Ic is related to upd of Cu on Rh, whereas peaks I'a and I"a are associated with the anodic stripping of upd Cu[15, 16]. On the other hand, peaks IIc and IIa correspond to the electrodeposition and electrodissolution of bulk Cu, respectively. The assignment of peaks Ic, I'a and I"a to different stages of upd Cu on Rh is confirmed by properly changing the voltammetry range in order to avoid the interference of bulk Cu electrodeposits (Fig. 5b). In this way, the similarity of upd Cu on Rh and pc Pt in acids[15, 17] suggests that peaks I'a and I"a can be assigned to the stripping of the weakly and strongly bound Cu, respectively.

The first voltammogram of Cu electrodeposition made on posc Rh (Fig. 6a) shows peak Ic at 0.30 V followed by the limiting cathodic current related to

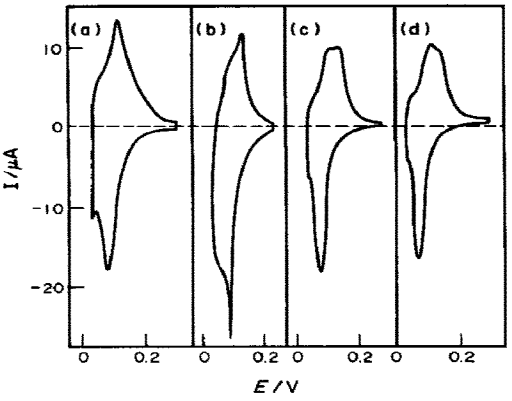

Fig. 4. (a) Voltammogram (1st scan) for a pfsc Rh electrode, $v = 0.1\ V\ s^{-1}$; $E_{s,c} = 0.03$ V, $E_{s,a} = 0.3$ V; 0.5 M H_2SO_4. (b) Voltammogram (1st scan) for a posc Rh electrode, $v = 0.1\ V\ s^{-1}$; $E_{s,c} = 0.03$ V, $E_{s,a} = 0.3$ V; 0.5 M H_2SO_4. (c) Voltammogram (8th scan) under conditions given for Fig. 4b. (Electrode area: 0.046 cm^2). (d) Voltammogram (10th scan) under conditions given for Fig. 4b. (Electrode area: 0.05 cm^2).

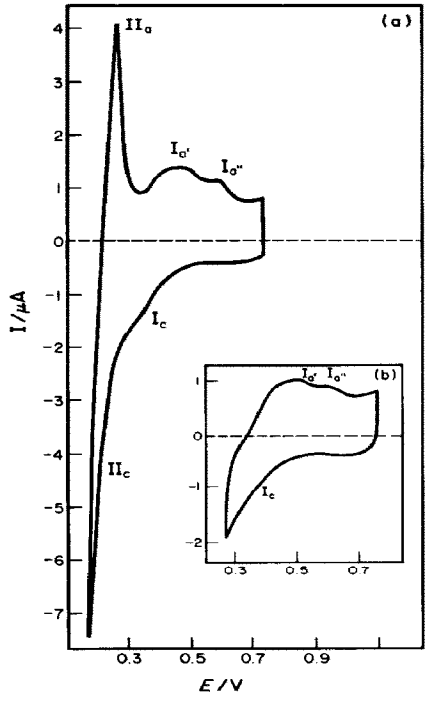

Fig. 5. (a) Voltammogram (1st scan) for a pfsc Rh electrode, $v = 0.02\ V\ s^{-1}$; $E_{s,a} = 0.75$ V, $E_{s,c} = 0.17$ V; 0.5 M H_2SO_4 + 10^{-3} M $CuSO_4$. (Electrode area: 0.04 cm^2). (b) Voltammogram (2nd scan) for a pfsc Rh electrode, $v = 0.02\ V\ s^{-1}$; $E_{s,a} = 0.75$ V, $E_{s,c} = 0.26$ V; 0.5 M H_2SO_4 + 10^{-3} M $CuSO_4$.

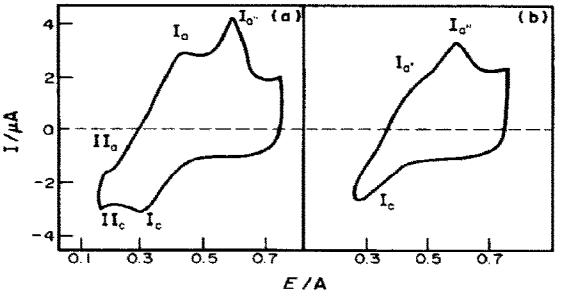

Fig. 6. (a) Voltammogram (1st scan) for a posc Rh electrode, $v = 0.02\ V\ s^{-1}$; $E_{s,a} = 0.75$ V, $E_{s,c} = 0.17$ V; 0.5 M H_2SO_4 + 10^{-3} M $CuSO_4$. (Electrode area: 0.04 cm^2). (b) Voltammogram (2nd scan) for a posc Rh electrode, $v = 0.02\ V\ s^{-1}$; $E_{s,a} = 0.75$ V, $E_{s,c} = 0.26$ V; 0.5 M H_2SO_4 + 10^{-3} M $CuSO_4$.

bulk Cu deposition (IIc). The latter is small as compared to that of the pfsc Rh (Fig. 5a). Therefore, peak IIa corresponding to the stripping of bulk Cu appears as a hump at 0.27 V mounted on the electrodeposition current. This result indicates that bulk Cu deposition is to a large extent inhibited on posc Rh, in coincidence with previously reported data on Rh (100) sc[6]. The second voltammetric scan made from $E_{s,c} = 0.26$ V to avoid bulk Cu deposition (Fig. 6b) is remarkably different from that recorded for pfsc Rh in the same potential range (Fig. 5b). In this case, the height of peak I″a is substantially increased and well-defined at 0.60 V, whereas peak I′a appears as a shoulder at the negative potential side (0.45 V). As observed for the H-atom electroadsorption–electrodesorption, the increase in the relative contribution of strongly bound Cu to weakly bound Cu gives further support to the predominant contribution of the (100) faces of posc Rh. These results resemble previously data reported for the upd of Cu on both Pt (100)[18, 19] and Rh (100) electrodes[6].

Acknowledgements—This work was financially supported by the Consejo Nacional de Investigaciones Cientificas y Técnicas and the Comisión de Investigaciones Científicas de la Provincia de Buenos Aires.

Authors are indebted to Dr M. Ipohorski for the facilities given for the SEM patterns.

REFERENCES

1. J. F. Llopis and I. M. Tordesillas, in *Encyclopedia of Electrochemistry of the Elements*, (Edited by A. J. Bard) Vol. VI, Marcel Dekker, New York (1976).
2. W. Böld and M. Breiter, *Electrochim. Acta* **5**, 169 (1961).
3. M. Brieter, *Electrochim. Acta* **7**, 25 (1962).
4. C. Pallotta, N. R. de Tacconi and A. J. Arvia, *Electrochim. Acta* **26**, 261 (1981).
5. A. M. Meretskii, I. V. Kudryashov and Yu. B. Vassilyev, *Elektrokhimiya* **13**, 447 (1977).
6. A. S. Lapa, V. A. Safonov, O. A. Petrii and N. L. Korenovskii, *Soviet Electrochemistry* **20**, 1439 (1984).

7. E. Custidiano, A. C. Chialvo, M. Ipohorski, S. Piovano and A. J. Arvia, *J. electroanal. Chem.* **221,** 229 (1987).
8. A. J. Arvia, J. C. Canullo, E. Custidiano, C. L. Perdriel and W. E. Triaca, *Electrochim. Acta* **31,** 1359 (1986).
9. J. Clavilier, R. Faure, G. Guinet and R. Durand, *J. electroanal. Chem.* **107,** 205 (1980); J. Clavilier, Thèse, Paris (1968).
10. R. Wood, in *Electroanalytical Chemistry* (Edited by A. J. Bard), Vol. 9, p. 1. Marcel Dekker, New York (1977).
11. G. Bélanger and A. K. Vijh, in *Oxides and Oxides Films,* (Edited by A. K. Vijh) Vol. 5, p. 1. Marcel Dekker, New York (1977).
12. J. C. Canullo, W. E. Triaca and A. J. Arvia, *J. electroanal. Chem.* **200,** 397 (1986).
13. B. Lang, R. W. Loyner and G. A. Somorjai, *Surf. Sci.* **30,** 440 (1972).
14. C. L. Perdriel, W. E. Triaca and A. J. Arvia, *J. electroanal. Chem.* **205,** 279 (1986).
15. B. Parajón Costa, C. D. Pallotta, N. R. de Tacconi and A. J. Arvia, *J electroanal. Chem.* **145,** 189 (1983).
16. R. O. Lezna, B. Beden and C. Lamy, *CR Acad. Sci. Paris, Serie II* **300** (1985).
17. C. L. Scortichini, F. E. Woodward and C. N. Reilley, *J. electroanal. Chem.* **139,** 265 (1982).
18. C. L. Scortichini and C. N. Reilley, *J. electroanal. Chem.* **139,** 233 (1982).
19. D. M. Kolb, R. Kotz and K. Yamamoto, *Surf. Sci.* **87,** 20 (1979).